The Spin Dependence of the Spatial Size of Fe(II) and of the Structure of Fe(II)-Porphyrins

5 AUTHORS, INCLUDING:

Andreas Dreuw
Universität Heidelberg
154 PUBLICATIONS   6,753 CITATIONS

SEE PROFILE

Russell J Boyd
Dalhousie University
304 PUBLICATIONS   6,008 CITATIONS

SEE PROFILE

The Spin Dependence of the Spatial Size of Fe(II) and of the Structure of Fe(II)-Porphyrins

Jesus M. Ugalde,*,§ Barry Dunietz,[†] Andreas Dreuw,[†] Martin Head-Gordon,[†] and Russell J. Boyd[‡]

*Kimika Fakultatea, Euskal Herriko Unibertsitatea, PK 1072, 20018 Donostia, Euskadi (Spain),
Department of Chemistry, University of California, Berkeley and Chemical Science Division,
Lawrence Berkeley National Laboratory, Berkeley, California 94720, and Department of Chemistry,
Dalhousie University, Halifax, N.S., B3H 4J3 Canada*

The question of why the iron displacement out of the porphyrin plane is enhanced in quintet states of singly ligated iron-porphyrin complexes compared to lower spin states and unligated iron-porphyrin is addressed. The spatial size of the Fe^{2+} atom is analyzed with respect to different spin states, and it is shown that the ion size decreases with increasing spin state for the d^6 electronic configuration. This contradicts the common belief that the iron out-of-plane location in the quintet state of ligated Fe(II)-porphyrins is due to an increased required space of the iron within the porphyrin ring. Therefore, the singlet, triplet, and quintet ground states of imidazole-ligated iron-porphyrin have been calculated employing density functional theory, and the relevant molecular orbitals have been analyzed. Additional comparison with the unligated iron-porphyrin molecules reveals that the enhanced doming in the quintet state is the result of a combination of the weakening of the iron-ring nitrogen bonds by occupying antibonding orbitals and the repulsion between the imidazole ligand and the porphyrin ring.

I. Introduction

The relationship between spin state and structure of Fe(II)-porphyrins (P) constitutes an active research topic due to its implications for the biological activity of heme proteins.[1,2] In particular, the role of doming of the FeP plane for the functionality of the proteins has been highlighted.[2,3] It is well established from the available experimental crystallographic data that high-spin Fe(II)-porphyrin complexes possessing an additional axial ligand, that is, the iron atom is pentacoordinated, are domed. In such high-spin complexes the iron atom is displaced ∼0.4 Å with respect to the porphyrin plane, while Fe(II)-porphyrin complexes with two additional ligands, in which the iron has an octahedral coordination sphere, exhibit essentially planar structures.[4−9] In low-spin states of either coordination type, the iron atom prefers essentially in-plane positions. Spectroscopic studies confirm these results. For instance, spectroscopic observations of protein dynamics occurring upon ligand dissociation have aided understanding the role of the doming mode for the protein functionality.[10−13] Similar structural features have also been observed for non-transition metal-porphyrins such as Pb(II)- and Sn(II)-porphyrins.[14]

The doming effect in Fe(II)-porphyrins is frequently explained by invoking atom-size considerations, since it is generally assumed that atomic high-spin states are spatially more extended than low-spin states. According to this argument an allegedly larger size of the iron atom in a high-spin state and the limited space of the iron in the porphyrin ring are associated with the out-of-plane movement of the iron, when pentacoordinated Fe(II)P complexes are promoted from low-spin to high-spin

states.[3,15−19] However, it has been shown theoretically[20] and confirmed experimentally[21] that high-spin states are not necessarily larger relative to lower spin states of the same atomic configuration. An alternative explanation is based on analysis of the orbital occupation. Semiempirical descriptions such as ligand field theory have been shown to provide a successful qualitative prediction of physical and chemical trends of related systems.[22,23] Specifically, the occupation of the iron $d_{x^2−y^2}$ orbital (involving electronic densities centered on the iron and oriented toward the lone pairs of the porphyrin ligating nitrogens) only in the high-spin states has been widely accepted as being responsible for the expansion of the core of ligated porphyrins. However, when considering the iron atom location with respect to spin state a higher quantitative description of the electronic system is needed. In this study we present an orbital occupation analysis based on ab initio calculations relevant for this aim.

In this paper we first estimate the spatial sizes of various spin states of Fe^{2+} by means of their calculated electron density distribution functions and their associated moments of the electron−nucleus distance, which provide a direct measure of the size of the atom.[24] In fact the atomic radius decreases with increasing spin state, and thus, the described atom-size argument for the out-of-plane movement of the iron atom in Fe(II)-porphyrin complexes is incorrect. Therefore, we further explore the origins of the iron displacement in the high-spin quintet state of an Fe(II)-porphyrin that is additionally ligated by an axial imidazole ligand (FePIm). We provide an explanation based on an analysis of the occupied orbitals of its singlet (low spin), triplet (intermediate spin), and quintet (high spin) states and a comparison to the unligated Fe(II)-porphyrin (FeP).

§ Euskal Herriko Unibertsitatea.
† University of California.
‡ Dalhousie University.

4654 *J. Phys. Chem. A, Vol. 108, No. 21, 2004*

Ugalde et al.

TABLE 1: Relative Energy ΔE (eV) with Respect to the ^{5}D ($3d^6$) Ground State (Experimental Values Are Given in *Italics*), the Systems-Averaged Density $\langle \rho \rangle$ (au), and Selected Moments of the Electron−Nucleus Distance (au), for Various Electronic States of Fe^{2+}

	^{5}D ($3d^6$)	^{3}P ($3d^6$)	^{3}G ($3d^6$)	^{1}I ($3d^6$)	^{7}S ($3d^54s^1$)
ΔE^a	0.000	2.508	2.733	3.935	4.320
	0.000	*2.406*	*3.045*	*3.764*	*3.730*
$\langle \rho \rangle$	4016.989	4017.130	4017.126	4017.206	4022.804
$\langle r^{-2} \rangle$	3182.527	3182.563	3182.559	3182.579	3184.653
$\langle r^{-1} \rangle$	114.906	114.889	114.886	114.878	114.666
$\langle r^1 \rangle$	15.282	15.316	15.320	15.337	16.159
$\langle r^2 \rangle$	16.194	16.306	16.321	16.381	19.907
$\langle r^3 \rangle$	23.102	23.434	23.480	23.658	36.578

^{a} E (^{5}D) $= -1262.80431265$ au.

II. Results and Discussion

First, we have calculated the spatial size of the Fe^{2+} ion to evaluate the previously described atom-size argument. The $3d^6$ electronic configuration of Fe^{2+} exhibits three spin states, namely, $S = 0$, $S = 1$, and $S = 2$, which correspond to the singlet, triplet, and quintet multiplicities, respectively. The ground state is known to be the ^{5}D state, then four triplets follow, the ^{3}P, ^{3}H, ^{3}F, and ^{3}G states. All these states have the $3d^6$ electronic configuration. The next stable state belongs to the $3d^54s^1$ configuration, namely, the ^{7}S state, which precedes the ^{1}I state. The latter state belongs again to the $3d^6$ electronic configuration. Their relative energies have been tabulated by Corliss and Sugar.[25]

We have calculated the B3LYP[26,27] Kohn−Sham orbitals[28,29] $\{\psi_i\}$, with GAMESS-UK,[30] of a selected set of these atomic states in order to obtain the electron density function, $\rho(\mathbf{r})$, as

$$\rho(\mathbf{r}) = \sum_i^N \psi_i^*(\mathbf{r})\psi_i(\mathbf{r}) \tag{1}$$

The basis set used for the iron was that given by Schäfer, Hurbert, and Ahlrichs,[31] supplemented with a diffuse s function (with an exponent 0.33 times that of the most diffuse s function on the original set), two sets of p functions optimized by Wachters[32] for the excited states, one set of diffuse d functions (optimized by Hay),[33] and three sets of uncontracted f functions, including both tight and diffuse exponents, as recommended by Raghavachari and Trucks.[34]

Then by following the algorithm of Sarasola et al.,[35] the electron density is used to calculate the system-averaged electron density

$$\langle \rho \rangle = \int \rho^2(\mathbf{r})\, d\mathbf{r} \tag{2}$$

and the moments of the electron−nucleus distance

$$\langle r^n \rangle = 4\pi \int_0^\infty \bar{\rho}(r) r^{n+2}\, dr \tag{3}$$

where $\bar{\rho}$ is the spherically averaged electron density:

$$\bar{\rho}(r) = \int \frac{d\Omega_{\mathbf{r}}}{4\pi} \rho(\mathbf{r}) \tag{4}$$

The results are listed in Table 1. We have also calculated the radial electron density distribution function, $4\pi r^2\bar{\rho}(r)$, for all the states listed in Table 1. These functions are plotted in Figure 1 with respect to the electron−nucleus distance, r.

Inspection of the data of Table 1 reveals that the size of the atom indeed depends on its spin state. Consider, for example,
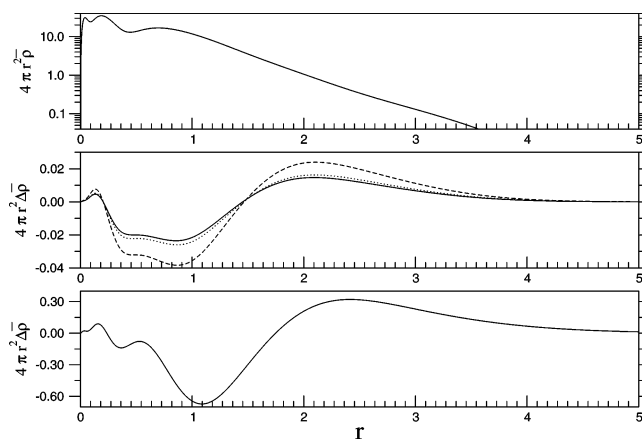

Figure 1. Upper panel: the electron density distribution function (au) for the ^{5}D ($3d^6$) ground state of Fe^{2+}. Middle panel: the incremental electron density distributions of the ^{3}P ($3d^6$, solid line), ^{3}G ($3d^6$, dotted line), and ^{1}I ($3d^6$, dashed line) states relative to the ^{5}D ($3d^6$) state. Lower panel: the incremental electron density distribution of the ^{7}S ($3d^54s^1$) state relative to ^{5}D ($3d^6$) state.

the $3d^6$ electronic configuration. When the mean electron−nucleus distances ($\langle r \rangle$) is inspected, it is demonstrated that the atomic size *decreases* with increasing spin multiplicity. Such size differences have been rationalized by the quantum mechanical explanation of Hund's rule.[36] Notice that moments $\langle r^2 \rangle$ and $\langle r^3 \rangle$ show the same trend. The same trend is also observed with the system-averaged electron density. Namely, the system-averaged electron density decreases with the spin multiplicity for states belonging to the same electronic configuration. Concomitantly, for the spin multiplicities with smaller atomic size (i.e., larger spin multiplicity) we found, as expected, larger values for the electron−nucleus attraction energy, that is, $E_{eN} = -Z\langle r^{-1} \rangle$, with Z being the iron's nuclear charge. The higher negative moment (-2), which emphasizes the short range region exhibits the opposite trend.

The electron density distribution function for the ^{5}D ($3d^6$) ground state of Fe^{2+} in Figure 1 is shown to decay logarithmically for large electron−nucleus distances. This mimics the exact decay behavior of the electron density distribution function.[37] Thus, it provides validation for the accuracy of our calculated approximate densities, at least in the long r region.

The electron density distributions of the calculated four electronic states with the $3d^6$ configuration nearly superimpose each other, as suggested by the small values of their incremental electron density distribution, $4\pi r^2\Delta\bar{\rho}$, shown in the middle panel of Figure 1. Nevertheless, it is worth pointing out that the ^{1}I ($3d^6$) state expands over larger radial electron−nucleus distances relative to the quintet ground and all the calculated triplets, since it drags more electron density out from the intermediate values of r over larger electron−nucleus distances. Focusing on the region close to the nuclei reveals reversal of the trend. For negative moments equal to (-2) (see Table 1) or larger (not reported) the trend is reversed. Indeed, inspection of the middle panel of Figure 1 reveals that near the nucleus at the small r values region, states with lower spin multiplicity exhibit higher densities. Since it is in this region where $\bar{\rho}$ acquires its largest values, both $\langle \rho \rangle$ and $\langle r^{-2} \rangle$ increase with decreasing spin multiplicity, as shown in Table 1. This is essentially a manifestation of the Fermi hole,[38,39] where the probability density of electrons of like spin to be found in the nearby proximity of each other is decreased. This permits lower multiplicity states to accumulate electron density close to the nucleus at the expense of intermediate electron−nucleus distance

Fe(II)-Porphyrin Spin States

J. Phys. Chem. A, Vol. 108, No. 21, 2004 **4655**
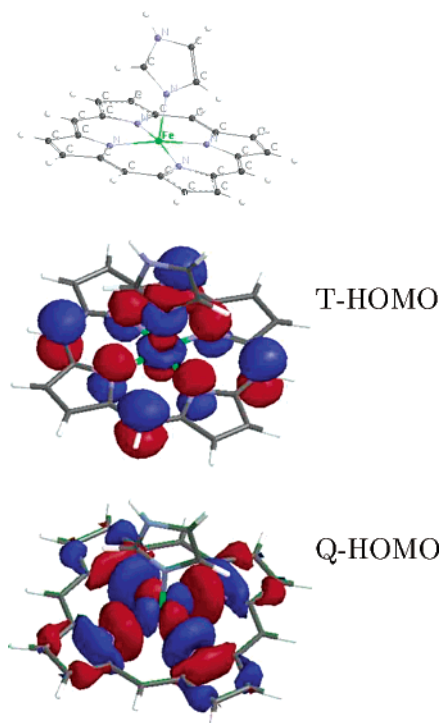
Figure 2. The molecular structure (top) as well as relevant molecular orbitals calculated at the equilibrium geometry of the singlet state are shown. The HOMO of the triplet state is depicted in the middle (T-HOMO), and the HOMO of the quintet state is provided in the bottom (Q-HOMO).

regions. This increased buildup of electron density near the nucleus for low-spin multiplicity states, with respect to the high-spin multiplicity states of the same configuration, increases the screening of the nuclear charge, and consequently, valence electrons span over large electron−nucleus distances. Hence, within the same electronic configuration, lower spin multiplicity states are bigger.[40]

The ^7S ($3d^54s^1$) state has a *more diffuse* electron density distribution (notice the large values of $4\pi r^2 \Delta\bar\rho$ in the lower panel of Figure 1). However, for this electronic configuration, the occupation of the 4s orbital renders a denser spherically averaged electron density, $\bar\rho$, near the nucleus, relative to the ^5D ($3d^6$) state, as shown in the lower panel of Figure 1. This screens the nuclear charge in such a way that the electron density turns out to be also denser away from the nucleus, at the expense of the substantially decreased electron density at intermediate values of r. This explains why both $\langle\rho\rangle$ and $\langle r^{-2}\rangle$ are largest for this state, while $\langle r^{-1}\rangle$ is the smallest of all the considered states. Note, this state was shown *not* to be present in the porphyrin environment. Extensive experimental[41] and theoretical investigations[42,43] have established beyond any reasonable doubt that the states of Fe^{2+} which play a role in Fe(II)-porphyrin complexes are the singlet, triplet, and quintet of the $3d^6$ electronic configuration.

Summarizing the calculations for the atomic spin states of Fe^{2+}, the spatial size of the ion decreases with increasing spin quantum number, that is, Fe^{2+} needs less space in a high-spin than in a low-spin state of the $3d^6$ electronic configuration. This clearly shows that the atom-size argument for the larger out-of-plane displacement of the iron atom in high-spin Fe(II)-porphyrin complexes is incorrect. To give an explanation, the structural effect is further investigated in the framework of Kohn−Sham density functional theory in the following paragraphs. Two molecular systems are studied, the unligated Fe(II)-porphyrin

TABLE 2: Different Spin States of Iron-Porphyrins in the Presence and the Absence of an Axial Ligand (Imidazole Group) Are Compared with Respect to Relative Energy and Iron Nitrogen Bond Distances[a]

model system	spin state	relative energy (kcal/mol)	out-of-plane displacement	bond length (Å)	
				Fe−N$_P$	Fe−N$_{Im}$
FePIm	singlet	7.3	0.16	2.005	1.925
	triplet	0.0	0.14	2.007	2.258
	quintet	2.8	0.36	2.100	2.173
FeP	singlet[b]		n/a		
	triplet	0.0	0.00	1.992	
	quintet	16.6	0.00	2.055	
Fe^{2+}	singlet	52.8			
	triplet	0.0			
	quintet	−39.0			

[a] The energies are provided relative to the triplet state and were calculated at the DFT/B3LYP/6-31G(d) level. Iron−nitrogen bond lengths are listed, where Fe−N$_P$ and Fe−N$_{Im}$ correspond to the distance from iron to nitrogen on the ring and to nitrogen on the axial ligand respectively. [b] The FeP singlet calculation does not converge. However, the results of FeP triplet and quintet are given, and they help to understand the effects underlying the iron location with respect to the molecular spin state of FePIm.

(FeP) and the imidazole-ligated FeP (FePIm) (Figure 2), of which the latter is a widely used model system for heme proteins, where the imidazole (Im) group mimics the histidine residue present in the real protein.

Our calculations comprise geometry optimizations of FeP and FePIm in their different spin ground states, the singlet, triplet, and quintet states, as well as the calculation and visualization of the molecular orbitals of these species. For this objective we employed standard ground-state density functional theory with the widely used B3LYP exchange-correlation functional[26,27] and the 6-31G(d) basis set. All molecular calculations have been performed using the QCHEM suite of programs.[44]

It has been reported that the B3LYP functional has a tendency to artificially prefer high-spin multiplicities.[45] However, this tendency is emphasized when comparing electronic states involving different valence shells. Hence, our results reported below, which focus on the comparison of d^6 electronic states, provide a reasonable level of accuracy. An additional confirmation for B3LYP adequacy is provided by the experience gained using B3LYP for studying related systems. These studies involve systems containing Fe atoms in general[46,47] and heme models in particular[18,43,48−50] and demonstrated the ability to reproduce relevant experimental data. These experimental observations involve the elongation of the ligand bonds upon axial ligation,[3,23,51] the relative stability of FeP different spin multiplicities states where the triplet state was found to be the most stable,[23,52,53] and most importantly the well-documented doming of the porphyrin ring associated with the iron located out of the plane for high-spin five-ligated systems.[23,51,54,55] Thus, models based on using the B3LYP functional are appropriate for the investigation at hand.

At their corresponding equilibrium geometries, the triplet state of FePIm is found to be the electronic ground state, while the quintet state is 2.8 kcal/mol higher in energy (see also Table 2). The singlet state is 7.3 kcal/mol higher in energy than the triplet. The calculated energy differences are slightly smaller than those found by Rovira et al.[18] For the unligated FeP molecule the triplet ground state is found to be 16.6 kcal/mol lower in energy than the quintet state in accord with previous calculations[18,43,48] (Table 2) and experimental data.[23] Unfortunately, the DFT calculation does not converge onto a stable solution for the singlet state. For the Fe^{2+} the correct ordering of the spin states (quintet, then triplet, and then singlet) is also

4656 *J. Phys. Chem. A, Vol. 108, No. 21, 2004*

Ugalde et al.

obtained with the 6-31G(d) basis set, as seen in Table 2. However, the relative energies among these spin states are poorer than those obtained with the considerably larger basis set used for the atomic calculations shown in Table 1.

The preference for the triplet states in the molecular systems versus the quintet state in the Fe^{2+} ion is a result of the competition between two major energetic effects. While high-spin states are energetically favored according to Hund's rule, molecular orbital theory, on the other hand, predicts lower stability for high-spin states since antibonding, energetically high-lying molecular orbitals become occupied. Later, the latter effect will be illuminated in detail.

The optimization of the geometries of the different spin states of FePIm revealed that the iron atom is slightly out-of-plane even for the singlet and triplet states by about 0.16 and 0.14 Å, respectively. This is in agreement with previous calculations by Rovira et al.[18] For the quintet state of FePIm we found the iron displaced out of the plane by 0.36 Å toward the imidazole ring (Table 2). In the unligated FeP molecule the iron atom has been found to be located within the plane of the porphyrin ring. Inspection of the optimized bond lengths of iron to the nitrogen atoms of the porphyrin ring (N_P) reveals that the $Fe-N_P$ bond distance increases from 2.01 Å in the low-spin states (singlet and triplet) to 2.1 Å in the quintet state. The bond length between iron and the imidazole nitrogen $Fe-N_{Im}$ increases with the spin multiplicity from 1.925 Å in the singlet to 2.258 Å in the triplet state and decreases again to be 2.173 Å in the quintet state (see Table 2). Smaller changes in the $Fe-N_P$ bond lengths but with a similar trend are observed for FeP when going from the triplet to the quintet state. The large increase of the $Fe-N_P$ distances from the triplet to the quintet state in the FePIm system clearly demonstrates the doming effect.

To explain the observed energetic and structural trends in the FePIm and FeP complexes, we have calculated the Kohn–Sham molecular orbitals (MOs) of the different spin states at the same planar geometry of the optimized singlet system (use of the optimized structure at higher multiplicities does not change the analysis). This allows us to directly inspect the orbital occupation which promotes the break of the structure planarity mainly at the high-spin state of FePIm. In principle, the transition from singlet to triplet can be seen as the promotion of an electron from a doubly occupied singlet MO to a virtual MO and, analogously, from the triplet to the quintet. The MOs which are additionally occupied in the triplet and quintet compared to the singlet state should thus explain the observed structural changes. These MOs are displayed in Figure 2, which correspond to the two highest singly occupied MOs of the quintet state at the equilibrium structure of the singlet state.

In analyzing the character of these open shell orbitals, we follow the widely used notation in the porphyrin literature. Accordingly, in assigning the symmetry of the orbitals, we have considered only the immediate environment of the iron atom and thus assume the system obeys the D_{4h} point group symmetry. In the following, we will focus on the orbitals which are occupied only in open shell spin occupation. These open shell orbitals describe antibonding interactions between the central iron atom and the ligands. Their corresponding bonding MOs are doubly occupied in all the spin multiplicities.

The highest occupied orbital (in the high-spin state) is denoted Q-HOMO in the figure. The high-spin configuration involves the occupation of the iron d-orbital ($d_{x^2-y^2}$), which introduces electronic lobes oriented toward the nitrogens of the ligated porphyrin. Here we choose the x and y axes to lie in the plane of the porphyrin ring and along the Fe–N bonds. This orbital,

denoted Q-HOMO in the figure, in the molecular environment of the porphyrin describes antibonding interactions of the iron with the nitrogens of the porphyrin ligands. This orbital is also frequently denoted as σ^*_{xy}.

The second highest occupied orbital of high-spin FeImP, through to the actual reduced symmetry of the system, involves mixing the iron d_{z^2} orbital and the HOMO of the porphyrin–semi-a_{2u}. This introduces antibonding interactions between the iron and the axial Im ligand. This orbital was found to be the HOMO of the triplet state and is denoted T-HOMO in the figure.

At the singlet state, the two highest occupied MOs correspond to pure Fe d-orbitals (not shown), and the depicted orbitals T-HOMO and Q-HOMO are unoccupied and have no energetic or structural effects. Orbital Q-HOMO, for example, corresponds to the sixth lowest unoccupied MO of the singlet state. Turning to the triplet state one electron is promoted to orbital T-HOMO. The orbital Q-HOMO of Figure 2 remains unoccupied in the triplet state and corresponds to its fourth lowest unoccupied orbital. In the quintet state yet another electron is promoted from a doubly occupied orbital of the triplet state into the former unoccupied orbital Q-HOMO. Here orbital T-HOMO corresponds to the Q-HOMO-1. Changing the spin state from singlet to triplet and quintet leads to substantial orbital relaxation effects and stabilization of Q-HOMO. Thereby, the formerly sixth lowest unoccupied MO of the singlet state becomes the HOMO of the quintet (Q-HOMO) without changing the spatial character of the orbital.

As described above, orbital T-HOMO exhibits strong antibonding character along the $Fe-N_{Im}$ bond, but introduces smaller antibonding effects with respect to the $Fe-N_P$ bonds. This explains why the $Fe-N_{Im}$ bond is elongated in the triplet compared to the singlet, while the $Fe-N_P$ bonds remain essentially constant. However, in both singlet and triplet states the iron is slightly displaced out of the porphyrin plane due to the ligand–ligand repulsion between the imidazole and the porphyrin ring. Thus the occupation of this orbital cannot explain the enhanced doming observed for the quintet state of FePIm. In the triplet this repulsion is reduced owing to an increased $Fe-N_{Im}$ bond, and as a consequence, the iron moves a little bit further in plane (see Table 2).

Orbital Q-HOMO has antibonding character with respect to the $Fe-N_P$ bonds, thus, it is responsible for the increase of the $Fe-N_P$ bond length in the quintet state relative to the triplet and singlet states. This explanation also holds for the unligated FeP molecule, since a similar orbital has been found to be the Q-HOMO. The occupation of this orbital, and the resulting weakening of the $Fe-N_P$ bonds, explains the reduced energy penalty calculated for the iron out-of-plane movement in the FeP system with increasing spin multiplicity.[18,48] Here, it is important to emphasize, however, that this orbital, which is occupied in the high-spin states of both considered systems, cannot be used solely to explain the pronounced out-of-plane motion observed only for the FeImP molecule.

However, the occupation of Q-HOMO in the quintet state of FePIm is clearly relevant for the enhanced doming of the iron–nitrogen plane. We have seen previously that the iron is also slightly displaced in the singlet and triplet states of FePIm by about 0.15 Å toward the imidazole ligand. The origin of this could only be the P–Im repulsion, because neither state of the unligated FeP is domed, since the planarity maximizes the bonding interactions between the iron and the porphyrin ring. The weakening of the $Fe-N_P$ bonds in the FePIm quintet state by occupation of the antibonding Q-HOMO (Figure 2) simply allows the P–Im repulsion to pull the iron atom further out.[56]

Fe(II)-Porphyrin Spin States

J. Phys. Chem. A, Vol. 108, No. 21, 2004 **4657**

The importance of the repulsion interactions is well demonstrated by considering replacing the axial ligand by a compact NH_2 amine group. For such simplified model systems a reduced out-of-plane iron location has been experimentally[23] and computationally[43] found. Hence in the quintet state the doming effect allows the reduction of the P—Im repulsion interactions, and the Fe—N_{Im} is allowed to relax and to become slightly shorter in the quintet than in the triplet state of FePIm. Thus, the enhanced doming of FePIm in the quintet state is a combined result of the repulsion between the Im ligand and the porphyrin ring and the weakening of the Fe—N_P bonds introduced by the high spin—orbital occupation.

III. Conclusions

In summary, our calculations have shown that the spatial size of the Fe^{2+} ion decreases with increasing spin multiplicity. Consequently, the argument that the enhanced doming of the Fe—N plane in the quintet state of FePIm is simply due to an increased required space of the Fe atom is wrong. In fact, analysis of the relevant molecular orbitals of FePIm and comparison with the unligated FeP molecule have clearly shown that the enhanced doming of FePIm when going from the singlet or triplet to the quintet state is the result of a combination of weakening the Fe—N_P bonds by occupation of an antibonding orbital and the P—Im ligand—ligand repulsion.

Supporting Information Available: Cartesian coordinates of all the optimized structures. This material is available free of charge via the Internet at http://pubs.acs.org.

References and Notes

(1) Lever, A. B. P.; Gray, H. B. *Iron Porphyrins*; Addison-Wesley: Reading, U.K., 1983.
(2) Perutz, M. F.; Wilkinson, A. J.; Paoli, M.; Dodson, G. G. *Annu. Rev. Biophys. Biomol. Struct.* **1998**, *27*, 1.
(3) Perutz, M. F. *Nature* **1970**, *726*, 228.
(4) Perutz, M. F. *Annu. Rev. Biochem.* **1979**, *48*, 327.
(5) Phillips, S. E.; Shoenborn, B. P. *Nature* **1981**, *292*, 81.
(6) Schlichting, I.; Berendzen, J.; Phillips, G. N., Jr.; Sweet, R. M. *Nature* **1994**, *371*, 808.
(7) Teng, T. Y.; Srajer, V.; Moffat, K. *Nat. Struct. Biol.* **1994**, *1*, 701.
(8) Hartmann, H.; Zinser, S.; Komninos, P.; Schneider, R. T.; Nienhaus, G. U.; Parak, F. *Proc. Natl. Acad. Sci. U.S.A.* **1996**, *93*, 7013.
(9) Srajer, V.; Teng, T. Y.; Ursby, T.; Pradervand, C.; Ren, Z.; Adachi, S.; Schildkamp, W.; Bourgeois, D.; Wulff, M.; Moffat, K. *Science* **1996**, *274*, 1726.
(10) Findsen, E. W.; Scott, T. W.; Chance, M. R.; Friedman, J. M.; Ondrias, M. R. *J. Am. Chem. Soc.* **1985**, *107*, 3355.
(11) Martin, J. L.; Migus, A.; Poyart, C.; Lecarpentier, Y.; Astier, R.; Antonetti, A. *Proc. Natl. Acad. Sci. U.S.A.* **1983**, *80*, 173.
(12) Lim, M.; Jackson, T. A.; Anfinrud, P. A. *Proc. Natl. Acad. Sci. U.S.A.* **1993**, *90*, 5801.
(13) Franzen, S.; Bohn, B.; Poyart, C.; Martin, J.-L. *Biochemistry* **1995**, *34*, 1224.
(14) Yamaki, T.; Nobusada, K. *J. Phys. Chem. A* **2003**, *107*, 2351.
(15) Hoard, J. In *Hemes and Hemoproteins*; Chance, B., Estabrook, R., Yonetane, T., Eds.; Academic Press: New York, 1966; pp 9—24.
(16) Hoard, J. *Science* **1971**, *174*, 1295.
(17) Kaim, W.; Schwederski, B. *Bioinorganic Chemistry: Inorganic Elements in the Chemsitry of Life*; J. Wiley and Sons: New York, 1994.
(18) Rovira, C.; Kunc, K.; Hutter, J.; Ballone, P.; Parrinello, M. *J. Phys. Chem. A* **1997**, *101*, 8914.
(19) Dreuw, A.; Dunietz, B. D.; Head-Gordon, M. *J. Am. Chem. Soc.* **2002**, *124*, 12070.
(20) Boyd, R. J. *Nature* **1974**, *250*, 566.
(21) Pichou, F.; Huetz, A.; Joyez, G.; Landau, M.; Mazeau, J. *J. Phys. B* **1976**, *9*, 933.
(22) Eaton, W.; Hanson, L. K.; Stephens, P.; Sutherland, J.; Dunn, B. *J. Am. Chem. Soc.* **1978**, *100*, 4991.
(23) Scheidt, W. R.; Reed, C. A. *Chem. Rev.* **1981**, *81*, 543.
(24) Boyd, R. J. *J. Phys. B* **1976**, *10*, 2283.
(25) Corliss, C.; Sugar, J. *J. Phys. Chem. Ref. Data* **1982**, *11*, 135.
(26) Becke, A. D. *J. Chem. Phys.* **1993**, *98*, 1372.
(27) Becke, A. D. *J. Chem. Phys.* **1993**, *98*, 5648.
(28) Hohenberg, P.; Kohn, W. *Phys. Rev.* **1964**, *136*, 864.
(29) Kohn, W.; Sham, L. J. *Phys. Rev.* **1965**, *140*, 1133.
(30) Gamess-uk is a package of ab initio programs written by M. F. Guest, J. H. van Lenthe, J. Kendrick, K. Schoffel, and P. Sherwood with contributions from R. D. Amos, R. J. Buenker, H. J. J. van Dam, M. Dupuis, N. C. Handy, I. H. Hillier, P. J. Knowles, V. Bonacic-Koutecky, W. von Niessen, R. J. Harrison, A. P. Rendell, V. R. Saunders, A. J. Stone, D. J. Tozer and A. H. de Vries. The package is derived from the original GAMESS code due to M. Dupuis, D. Spangler, and J. Wendoloski, NRCC Software Catalog, Vol. 1, Program No. QG01 (GAMESS), 1980.
(31) Schäfer, A.; Hurbert, C.; Ahlrichs, R. *J. Chem. Phys.* **1994**, *100*, 5829.
(32) Wachters, A. J. *J. Chem. Phys.* **1970**, *52*, 1033.
(33) Hay, P. J. *J. Chem. Phys.* **1971**, *66*, 4377.
(34) Raghavachari, K.; Trucks, G. W. *J. Chem. Phys.* **1989**, *91*, 1062.
(35) Sarasola, C.; Elorza, J. M.; Ugalde, J. M. *J. Math. Chem.* **1998**, *23*, 405.
(36) Boyd, R. J. *Nature* **1984**, *310*, 480.
(37) Tal, Y. *Phys. Rev. A* **1978**, *18*, 1781.
(38) Boyd, R. J.; Coulson, C. A. *J. Phys. B* **1974**, *7*, 1805.
(39) Ludeña, E. V.; Ugalde, J. M.; Lopez, X.; Fernández-Rico, J.; Ramirez, G. *J. Chem. Phys.* **2004**, *120*, 540.
(40) Katriel, J. *Phys. Rev. A* **1972**, *5*, 1990.
(41) Spiro, T. G.; Zgierski, M. Z.; Kozlowski, P. M. *Coord. Chem. Rev.* **2001**, *219*, 923.
(42) Bersuker, I.; Stavrov, S. S. *Coord. Chem. Rev.* **1988**, *88*, 1.
(43) Kozlowski, P. M.; Spiro, T. G.; Bérces, A.; Zgierski, M. Z. *J. Phys. Chem. B* **1998**, *102*, 2603.
(44) Kong, J.; White, C. A.; Krylov, A. I.; Sherrill, D.; Adamson, R. D.; Furlani, T. R.; Lee, M. S.; Lee, A. M.; Gwaltney, S. R.; Adams, T. R.; Ochsenfeld, C.; Gilbert, A. T. B.; Kedziora, G. S.; Rassolov, V. A.; Maurice, D. R.; Nair, N.; Shao, Y.; Besley, N. A.; Maslen, P. E.; Dombroski, J. P.; Daschel, H.; Zhang, W.; Korambath, P. P.; Baker, J.; Byrd, E. F. C.; Van Voorhis, T.; Oumi, M.; Hirata, S.; Hsu, C.-P.; Ishikawa, N.; Florian, J.; Warshel, A.; Johnson, B. G.; Gill, P. M. W.; Head-Gordon, M.; Pople, J. A. *J. Comput. Chem.* **2000**, *21* (16), 1532—1548.
(45) Ricca, A.; Bauschlicher, C. W. *Chem. Phys. Lett.* **1995**, *245*, 150.
(46) Ricca, A.; Bauschlicher, C. W. *J. Phys. Chem.* **1995**, *99*, 5922.
(47) Dunietz, B.; Beachy, M.; Cao, Y.; Whittington, D.; Lippard, S.; Friesner, R. *J. Am. Chem. Soc.* **2000**, *122*, 2828.
(48) Spiro, T. G.; Kozlowski, P. M.; Zgierski, M. Z. *J. Raman Spectrosc.* **1998**, *29*, 869.
(49) McMahon, B.; Stojkovic, B.; Hay, P.; Martin, R.; Garcia, A. *J. Chem. Phys.* **2000**, *113*, 6831.
(50) Dunietz, B.; Dreuw, A.; Head-Gordon, M. *J. Phys. Chem. B* **2003**, *107*, 5623.
(51) Parthasarathi, N.; Hansen, C.; Yamaguchi, S.; Spiro, T. G. *J. Am. Chem. Soc.* **1987**, *109*, 3865.
(52) Collman, J.; Hoard, J.; Kim, N.; Lang, G.; Reed, C. *J. Am. Chem. Soc.* **1975**, *97*, 2676.
(53) Lang, G.; Spartalian, K.; Reed, C.; Colleman, J. *J. Chem. Phys.* **1978**, *69*, 5424.
(54) Jameson, G. B.; Mollinaro, F.; Ibers, J.; Colleman, J.; Brauman, J.; Rose, E.; Suslick, K. *J. Am. Chem. Soc.* **1980**, *102*, 3224.
(55) Choi, S.; Spiro, T. G.; Langry, K. C.; Smith, K. M.; Budd, D. L.; La Mar, G. N. *J. Am. Chem. Soc.* **1982**, *104*, 4345.
(56) Olafson, B. D.; Goddard, W. A. *Proc. Natl. Acad. Sci. U.S.A.* **1977**, *74*, 1315.